NACA TN No. 1505

8608

TECH LIBRARY KAFB, NM
0144640

NATIONAL ADVISORY COMMITTEE FOR AERONAUTICS

TECHNICAL NOTE

No. 1505

THE INWARD BULGE TYPE BUCKLING OF MONOCOQUE CYLINDERS

V - REVISED STRAIN ENERGY THEORY WHICH ASSUMES A MORE GENERAL DEFLECTED SHAPE AT BUCKLING

By N. J. Hoff, Bertram Klein,
and Bruno A. Boley

Polytechnic Institute of Brooklyn

Washington
September 1948

AFMDC
TECH
SEP 2011

NATIONAL ADVISORY COMMITTEE FOR AERONAUTICS

TECH LIBRARY KAFB, NM
0144640

TECHNICAL NOTE NO. 1505

THE INWARD BULGE TYPE BUCKLING OF MONOCOQUE CYLINDERS

V - REVISED STRAIN ENERGY THEORY WHICH ASSUMES A MORE GENERAL DEFLECTED SHAPE AT BUCKLING

By N. J. Hoff, Bertram Klein,
and Bruno A. Boley

SUMMARY

A strain energy theory is developed for the calculation of the critical load for the inward bulge type of general instability of reinforced monocoque cylinders subjected to pure bending. The deflected shape at buckling is assumed to be represented by an expression containing eight free parameters in addition to the two characterizing the wave lengths in the circumferential and axial directions. The theory is applied to two representative cylinders of the GALCIT test series and to two of the PIBAL series. The critical stresses calculated are 8.3 to 22.9 percent higher than the experimental values.

INTRODUCTION

When a reinforced aluminum-alloy monocoque fuselage is subjected to bending moments, such as those caused by the aerodynamic loads acting upon the tail surfaces, structural failure is likely to occur by the buckling of the stringers on the compression side of the fuselage. The half wave length of the deflected shape is equal to the spacing of the ring frames when the frames are comparatively rigid and are spaced far apart. The critical stress can be increased by spacing the rings closer, but at the same time the cross-sectional dimensions of the rings must be made smaller in order to keep the weight of the structure unchanged. Such a trend can be noticed in the development of the modern monocoque fuselage from 1930 until the present time. When, however, the distance between rings and the cross section of the ring decreases beyond a certain limit, the rings no longer have sufficient bending rigidity to act as rigid supports for the stringers. In such a case failure occurs by general instability in which several stringers and rings are involved simultaneously.

The general instability of a reinforced thin-walled curved shell was first investigated by Dschou in 1935 (reference 1) who, at the ggestion of H. Wagner, worked out and applied to monocoques the buckling ieory of

orthotropic shells established in 1932 by Flügge (reference 2). A similar theory was worked out independently by Taylor (reference 3) in 1935. In these investigations a uniformly distributed compressive loading was assumed. It was believed that the results would also apply in the case of bending provided that the wave length in the circumferential direction were small enough so that the variation in the intensity of the compressive stress caused by the bending moment could be disregarded. At the same time the wave length must be greater than the spacing of the reinforcing elements. Otherwise the structure cannot be considered as an orthotropic shell. The results of these theories were compared later with experiments carried out at GALCIT in 1939 (references 4 to 8). It was found that the buckling loads predicted were several times as high as those observed.

Another form of general instability, caused by bending, was investigated by Heck in 1937 (reference 9) whose work is a generalization and application to reinforced monocoques of an earlier theoretical analysis of Brazier in 1927 (reference 10). This type of instability consists of a flattening of the rings and is of no practical importance in aluminum-alloy reinforced monocoque fuselages.

The problem of general instability due to bending was approached from another angle by Hoff in 1938 (reference 11). The most highly compressed stringers were considered as columns elastically supported by the rings, and the buckling load was calculated by the strain energy method. The deflected shape was assumed to be mainly an inward bulge symmetric with respect to the most highly compressed stringer. The stringers were assumed to be distributed uniformly around the circumference but the rings were treated individually. The buckling load was minimized with respect to two parameters which were the lengths of the wave in the axial and the circumferential directions. Tests carried out with two cylinders showed that the inward bulge type of general instability was possible and that it occurred approximately at the stress predicted by theory. A nondimensional structural parameter Λ was found, the magnitude of which determined whether failure would occur by general or panel instability.

The extended experimental investigations undertaken at GALCIT beginning in 1938 proved Hoff's theory to be too conservative for practical use. In GALCIT's theoretical development Von Kármán and Tsien (reference 12) found that the classical linear theory had to be replaced by a nonlinear theory in order to predict correctly the buckling loads of nonreinforced cylinders. Because of the complexity of the nonlinear theory even in the case of nonreinforced cylinders the idea of finding a theoretical solution of the buckling problem of reinforced cylinders was given up at GALCIT. An empirical formula based on dimensional analysis was established which was in good agreement with the results of the GALCIT tests.

In 1943 Hoff (reference 13) published a new version of his theory. A review of his earlier work disclosed that there the circumferential wave length, not expressed explicitly, was always equal to the total circumference of the cylinder after the buckling load was minimized. On the

other hand, in the tests the inward bulge was restricted to the most highly compressed regions of the cylinder. In the new publication the discrepancy between experiment and theory was attributed to the fact that in the original work the shear strain energy stored in the sheet covering was neglected. On the other hand, the strain energy of shear was found to be unduly large when it was assumed that the expressions describing the distortions of the stringers and rings were valid also for the sheet. Apparently there are patterns of distortion for the sheet which involve less strain energy, particularly when the sheet is already in a buckled state at the moment when general instability occurs.

The difficulties involved in finding the actual distortions of the sheet covering were circumvented through a semiempirical approach. The wave-length parameter n was assumed so as to obtain an agreement between the buckling load observed in the GALCIT tests and the predictions of the theory. In reality the wave length must depend upon the variation of the shearing rigidity of the panels of sheet around the circumference of the cylinder, and the shearing rigidity is certainly influenced by the compressive and shearing stresses prevailing in the panels. It was concluded, therefore, that n was dependent upon two parameters characterizing the state of the sheet, namely r/d and $\epsilon_{max} r/t$. The connection between these two parameters and n was established from an evaluation of the GALCIT test results, and the correctness of the assumptions was substantiated by the fact that a family of smooth curves was obtained. With the aid of these curves the buckling load could be predicted in a simple manner.

The purely theoretical analysis was resumed in 1945 by Hoff and Klein (reference 14) at PIBAL. It was found that the shear strain energy stored in the sheet covering was not unreasonably large when it was calculated on the basis of an average shear angle defined by the relative displacements of the four corners of each panel. Such a treatment disregards details of the states of stress and strain in the panel and should be based on experimental values of the shearing rigidity of panels subjected to arbitrary compressive loads. In the absence of experimental data a connection between shearing rigidity and compressive load was assumed which was hoped to represent fairly the actual conditions. Other improvements upon the original treatment of the subject were the replacement of the expression defining the shape of the wave in the circumferential direction by a new expression which satisfied more rigorous boundary conditions and the replacement of the integration around the circumference by a summation. The new results were in good agreement with the GALCIT test data.

An experimental investigation of the shearing rigidity of reinforced monocoque cylinders carried out at PIBAL by Hoff and Boley (reference 15) in 1946, however, resulted in the measurement of considerably higher shearing rigidities than expected in the case of curved panels subjected to compressive loads exceeding the critical loads. The use of such high values of the shearing rigidity in the revised theory just discussed would have

resulted in buckling loads considerably larger than those observed. At this stage of the development the authors began to entertain some doubts whether the problem could be solved by a linear theory.

Their conviction that a linear theory would predict correctly the buckling load in general instability had been based on the following observations. The inward bulge proper was always restricted to a region of the cylinder where the sheet covering was in a buckled state when general instability occurred. Because of the increased movability of the wavy curved sheet the reinforced monocoque cylinder was reduced essentially to a grid consisting of stringers and rings connected somewhat loosely by the buckled sheet. The question arises now whether the support rendered by the rings to the stringers has a linear characteristic. In experiments carried out at PIBAL with reinforced monocoque cylinders a linear connection was found between a load applied radially to a ring and the deflection of the point of attack. Under such a load the entire ring distorted, whereas in tests undertaken at GALCIT in order to clarify some aspects of the nonlinear theory the nonlinear support was furnished by a semicircular element, the ends of which were rigidly fixed. In the general instability tests both at GALCIT and PIBAL the rings were observed to distort slightly around the entire circumference so that the end points of the main bulge were definitely not fixed. Because of these considerations one more attempt was made at PIBAL to explain the phenomenon of the inward bulge type of general instability by a linear theory. The results of this investigation are presented in the present report.

The strain energy method is known to yield too high buckling loads if the assumptions regarding the deflected shape deviate from the actual shape of deflections. An effort was made therefore to make the new assumptions more elastic than were the earlier ones by the use of a greater number of parameters that can adjust themselves in the process of minimization. Altogether nine free parameters were incorporated in the expression describing the deflected shape, one of which is indeterminate as in all buckling problems. To the remaining eight parameters may be added the two parameters defining the wave length in the circumferential and axial directions.

The strain energy and the work of the external forces were calculated by summation as in the earlier publication (reference 14), and in the determination of the shear strain energy stored in the sheet covering the experimentally obtained values of the shearing rigidity were used. The large number of parameters did not permit the development of an expression in closed form for the buckling load but four representative cylinders were investigated numerically and the calculations resulted in buckling stresses in satisfactory agreement with the test results. The authors believe that the agreement obtained between theory and experiment substantiates the claims for an essentially linear character of the problem in the form it was set up in these calculations. Details of the behavior of the buckled panels, however, cannot be explained in all

probability by a linear theory. It is quite likely that better agreement between theory and experiment can be obtained if an even more complicated, or else a better, shape is assumed for the deflections.

The calculations presented here are too lengthy for use in structural design. The writers believe that the simple formulas developed in reference 13 are those most suitable for practical calculations. The value of the parameter n should be taken from a diagram published by Hoff, Boley, and Nardo (reference 16), which is a revised version of the diagram presented in reference 13. The differences between the two diagrams are the incorporation of new test data obtained in a series of tests at PIBAL and the correction of the earlier test results for the effects of stresses exceeding the elastic limit. The importance of the theory presented in this report is twofold. First, it can be used in the calculation of n values in that region of the parameters r/d and $\epsilon_{max}r/t$ which is not easily accessible to experimental methods. In such a manner a more comprehensive n diagram can be constructed than the one available at present without recourse to a very extensive test program involving cylinders of the size of the fuselages of modern transport airplanes. Second, it establishes the fundamental soundness of the linear approach upon which the method suggested for practical calculations and the n diagram are based.

For the sake of completeness other publications dealing with general instability are now listed. In 1937 Nissen (reference 17) compared test results obtained with reinforced cylindrical panels and complete cylinders subjected to compression with Dschou's theory. Satisfactory agreement was found after an empirical factor was incorporated. Ryder (reference 18) attempted in 1938 to improve Taylor's theory by the use of empirical factors. In 1942 Tsun Kuei Wang (reference 19) developed a theory of the flattening of monocoque cylinders subjected to compression, but the applicability of his results is impaired by the fact that he neglected the shear strain energy stored in the sheet covering. At PIBAL additional theoretical investigations related to the inward bulge type instability were carried out by Hoff and Klein (reference 20) in 1944 and a series of cylinders was tested by Hoff, Fuchs, and Cirillo (reference 21) in the same year. A new general instability theory was worked out by Wang (reference 22) in 1946 in which the wave form was described by infinite series. The shear strain energy stored in the sheet was not calculated but its effect was taken into account by means of an empirical multiplying factor depending upon the size of the panels.

For his contribution to the calculations presented in the present report the authors are indebted to Merven W. Mandel. This investigation was conducted at the Polytechnic Institute of Brooklyn under the sponsorship and with the financial assistance of the National Advisory Committee for Aeronautics.

SYMBOLS

a_o	indeterminate coefficient
a,b,c,d,e,f,g,h	parametric coefficients
A	cross-sectional area of stringer plus effective width of sheet
A_{str}	area of stringer
d	width of panel measured along circumference
E	Young's modulus
E_{red}	reduced modulus
E_{sec}	secant modulus
E_{tan}	tangent modulus
G	shear modulus
G_o	shear modulus of sheet covering at zero compressive load
G_{eff}	effective shear modulus
h	centroidal height of stringer
i	index denoting position along circumference
I	moment of inertia
I_r	moment of inertia of ring cross section and its effective width of sheet for bending in its own plane
$I_{str_{ro}}$	moment of inertia of stringer cross section for bending in radial direction (about its tangential principal axis)
I_{str_r}	moment of inertia of stringer cross section and effective width of curved sheet for bending in radial direction (about its tangential principal axis)
$I_{str_{to}}$	moment of inertia of stringer cross section for bending in tangential direction (about its radial principal axis)
I_{str_t}	moment of inertia of stringer cross section and effective width of curved sheet for bending in tangential direction (about its radial principal axis)

j	index denoting position along axial direction
L	length of wave in axial direction
L_1	distance between adjacent rings
$m + 1$	number of ring fields involved in failure
M	function appearing in strain energy of bending of rings
n	parameter defining wave length in circumferential direction
P_1, P_2	polynomial functions of a,b,c,d,e,f,g, and h
P	force acting on stringer and its effective curved sheet at buckling
Q	function appearing in shear strain energy
r	radius of cylinder
s	number of stringer fields involved in bulge
S	total number of stringers in cylinder
t	thickness of sheet covering
U	strain energy
U_r	bending strain energy stored in rings
U_{sh}	shear strain energy stored in sheet
U_{str_r}	radial bending strain energy stored in stringers
U_{str_t}	tangential bending strain energy stored in stringers
$2w$	effective width of curved sheet
w_n	rotation of tangent of ring
w_r	radial displacement of a point on a ring or a stringer
w_t	tangential displacement of a point on a ring or a stringer
W	work done by applied forces at buckling
x	axial coordinate
α_n, α_r, α_t	coefficients used in calculation of shear strain in a panel due to rotations and displacements of its corners

β	angle subtended by a panel
γ	shear strain
δ	shift of neutral axis from horizontal diameter at buckling, percent of radius
ϵ	normal strain in a stringer plus its effective curved sheet at buckling
ϵ_{cr}	maximum compressive strain at buckling
$\epsilon_{cr_{sh}}$	compressive buckling strain of sheet panel
ϵ_{cu}	buckling strain of a nonreinforced circular cylinder under uniform axial compression
ϵ_{ft}	buckling strain of a flat panel of sheet in compression
Λ	structural buckling index
φ	angular coordinate
Φ_r	function of φ appearing in expression for w_r
Φ_t	function of φ appearing in expression for w_t

DEVELOPMENT OF A REVISED BUCKLING THEORY WHICH INCLUDES EIGHT ARBITRARY PARAMETERS

Revised Deflection Pattern

The shape of the bulge at buckling is determined mainly by the radial deflections. The following expression is chosen to represent the radial deflections w_r occurring at buckling:

$$w_r = a_o\left[\Phi_r(l,a,b)\,\sin^2(\pi x/L) + \Phi_r(c,d,e)\,\sin^6(\pi x/L) + \Phi_r(f,g,h)\,\sin^{10}(\pi x/L)\right] \tag{1}$$

provided that

$$\left.\begin{aligned} 0 \le \varphi \le (\pi/n) \\ 0 \le x \le L \end{aligned}\right\} \tag{1a}$$

where

$$\Phi_r(c,d,e) = \left[c \cos n\varphi + d \cos 2n\varphi + e \cos 3n\varphi \right.$$

$$+ (2.666...c - 2.333...d + 1.777...e) \cos 4n\varphi$$

$$\left. + (1.666...c - 1.333...d + 0.777...e) \cos 5n\varphi\right] \quad (1b)$$

The value of $\Phi_r(1,a,b)$ is obtained by replacing c, d, and e in equation (1b) by 1, a, and b, respectively; $\Phi_r(f,g,h)$ is obtained by replacing c, d, and e by f, g, and h, respectively.

Also $w_r = 0$ when $\varphi > \pi/n$ and/or $x > L$ (1c)

The notation and the sign conventions are shown in figure 1.

The deformations of the rings are assumed to be inextensional. The condition for inextensionality is:

$$w_r = - \partial w_t/\partial\varphi \quad (2)$$

Equations (1) and (2) determine the tangential deflections w_t:

$$w_t = - (a_o/n) \left[\Phi_t(1,a,b) \sin^2(\pi x/L) + \Phi_t(c,d,e) \sin^6(\pi x/L) \right.$$

$$\left. + \Phi_t(f,g,h) \sin^{10}(\pi x/L)\right] \quad (3)$$

provided that

$$\left.\begin{aligned} 0 \leq \varphi \leq (\pi/n) \\ 0 \leq x \leq L \end{aligned}\right\} \quad (3a)$$

where

$$\Phi_t(c,d,e) = \left[c \sin n\varphi + (1/2)\, d \sin 2n\varphi + (1/3)\, e \sin 3n\varphi \right.$$

$$+ (1/4)(2.666\ldots c - 2.333\ldots d + 1.777\ldots e) \sin 4n\varphi$$

$$\left. + (1/5)(1.666\ldots c - 1.333\ldots d + 0.777\ldots e) \sin 5n\varphi\right] \quad (3b)$$

The value of $\Phi_t(1,a,b)$ is obtained by replacing c, d, and e in equation (3b) by 1, a, and b, respectively; $\Phi_t(f,g,h)$ is obtained by replacing c, d, and e by f, g, and h, respectively.

Also $w_t = 0$ when $\varphi > \pi/n$ and/or $x > L$ (3c)

A few explanatory remarks are now given regarding the choice of the deflected shape. In order that the bulge be symmetric about the bottom stringer $\varphi = 0$ the following conditions must be satisfied there:

1. The tangential displacements must vanish:

$$w_t = 0 \quad \text{when} \quad \varphi = 0, \quad \text{for all values of} \quad x \qquad (4a)$$

and

2. The radial deflection pattern must exhibit a horizontal tangent:

$$\left(\partial w_r/\partial\varphi\right) = 0 \quad \text{when} \quad \varphi = 0, \quad \text{for all values of} \quad x \qquad (4b)$$

Further, in order that there be a smooth transition between the bulge and the nondistorted part of the cylinder at $\varphi = (\pi/n)$, the following conditions must be satisfied there:

3. The tangential displacements must vanish:

$$w_t = 0 \quad \text{when} \quad \varphi = (\pi/n), \quad \text{for all values of} \quad x \qquad (4c)$$

4. The radial displacements must vanish:

$$w_r = 0 \quad \text{when} \quad \varphi = (\pi/n), \quad \text{for all values of} \quad x \tag{4d}$$

5. There must be no sudden change in the direction of the tangent:

$$\left(\partial w_r/\partial \varphi\right) = 0 \quad \text{when} \quad \varphi = (\pi/n), \quad \text{for all values of} \quad x \tag{4e}$$

and

6. There must be no sudden change in the curvature:

$$\left(\partial^2 w_r/\partial \varphi^2\right) = 0 \quad \text{when} \quad \varphi = (\pi/n), \quad \text{for all values of} \quad x \tag{4f}$$

Finally, in order that there be a smooth transition between the bulge and the nondistorted part of the cylinder at $x = 0$ and $x = L$, the following conditions must be satisfied there:

7. The tangential displacements must vanish:

$$w_t = 0 \quad \text{when} \quad x = 0 \text{ (or L)}, \quad \text{for all values of} \quad \varphi \tag{4g}$$

8. The radial displacements must vanish:

$$w_r = 0 \quad \text{when} \quad x = 0 \text{ (or L)}, \quad \text{for all values of} \quad \varphi \tag{4h}$$

and

9. There must be no sudden change in the direction of the tangent:

$$\left(\partial w_r/\partial x\right) = 0 \quad \text{when} \quad x = 0 \text{ (or L)}, \quad \text{for all values of} \quad \varphi \tag{4i}$$

It can be shown that equations (1) and (3) satisfy all the boundary conditions enumerated in equations (4a) to (4i). (The arbitrary function of x which would normally appear in equation (3) as a result of the integration of equation (2) is zero as a consequence of condition (4a).) Typical examples of the deflection patterns of a stringer and a ring, taken from the results of the calculations, are shown in figures 2(a) and 2(b).

Calculation of Strain Energy

Strain energy stored in rings.- The strain energy stored in any one ring is

$$U = (1/2)\left[(EI)_r/r^3\right]\int_{-\pi/n}^{\pi/n}\left[w_r + \left(\partial^2 w_r/\partial\varphi^2\right)\right]^2 \partial\varphi \qquad (5)$$

If the value of w_r is substituted from equation (1) and the strain energy is summed over all the rings, the following expression is obtained:

$$U_r = (1/2)\left(a_o^2/r^3\right)\int_{-\pi/n}^{\pi/n}\left\{\left[\Phi_r(1,a,b) + \Phi_r^{11}(1,a,b)\right]\sum_{j=1}^{m}(EI)_r \sin^2\left(\pi x_j/L\right)\right.$$

$$+ \left[\Phi_r(c,d,e) + \Phi_r^{11}(c,d,e)\right]\sum_{j=1}^{m}(EI)_r \sin^6\left(\pi x_j/L\right)$$

$$\left.+ \left[\Phi_r(f,g,h) + \Phi_r^{11}(f,g,h)\right]\sum_{j=1}^{m}(EI)_r \sin^{10}\left(\pi x_j/L\right)\right\}^2 d\varphi \qquad (6)$$

where m is the total number of rings included in the wave length L. The integration yields a result in closed form. The summations contained in equation (6) can be evaluated algebraically as functions of $(m + 1)$. They are given in table I. If all the rings have the same bending rigidity $(EI)_r$, the total strain energy U_r stored in all the rings becomes

$$U_r = (1/2)\left(a_o^2/r^3\right)(EI)_r\pi\left[M(1,a,b)\sum_j \sin^4\left(\frac{\pi j}{m+1}\right) + M(c,d,e)\sum_j \sin^{12}\left(\frac{\pi j}{m+1}\right)\right.$$

$$+ M(f,g,h)\sum_j \sin^{20}\left(\frac{\pi j}{m+1}\right) + 2M\begin{pmatrix}1,a,b\\c,d,e\end{pmatrix}\sum_j \sin^8\left(\frac{\pi j}{m+1}\right)$$

$$\left.+ 2M\begin{pmatrix}1,a,b\\f,g,h\end{pmatrix}\sum_j \sin^{12}\left(\frac{\pi j}{m+1}\right) 2M\begin{pmatrix}c,d,e\\f,g,h\end{pmatrix}\sum_j \sin^{16}\left(\frac{\pi j}{m+1}\right)\right] \qquad (7)$$

where

$$M(c,d,e) = \left[(4n^2 - 1)^2 + (2.333\ldots)^2(16n^2 - 1)^2 + (1.333\ldots)^2(25n^2 - 1)^2\right] d^2$$

$$- 2\left[(2.333\ldots)(1.777\ldots)(16n^2 - 1)^2 + (1.333\ldots)(0.777\ldots)(25n^2 - 1)^2\right] de$$

$$+ \left[(9n^2 - 1)^2 + (1.777\ldots)^2 (16n^2 - 1)^2 + (0.777\ldots)^2(25n^2 - 1)^2\right] e^2$$

$$- 2\left[(2.666\ldots)(2.333\ldots)(16n^2 - 1)^2 + (1.666\ldots)(1.333\ldots)(25n^2 - 1)^2\right] cd$$

$$+ 2\left[(2.666\ldots)(1.777\ldots)(16n^2 - 1)^2 + (1.666\ldots)(0.777\ldots)(25n^2 - 1)^2\right] ce$$

$$+ \left[(n^2 - 1)^2 + (2.666\ldots)^2(16n^2 - 1)^2 + (1.666\ldots)^2(25n^2 - 1)^2\right] c^2 \qquad (7a)$$

The value of $M(1,a,b)$ is obtained by replacing c, d, and e by 1, a, and b, respectively; $M(f,g,h)$ is obtained by replacing c, d, and e by f, g, and h, respectively; $M\binom{1,a,b}{c,d,e}$ is obtained by replacing d^2 by ad, de by $(1/2)(ae + bd)$, e^2 by be, cd by $(1/2)(d + ac)$, ce by $(1/2)(e + bc)$, and c^2 by c; $M\binom{c,d,e}{f,g,h}$ is obtained by replacing d^2 by dg, de by $(1/2)(dh + eg)$, e^2 by eh, cd by $(1/2)(cg + df)$, ce by $(1/2)(ch + ef)$, and c^2 by cf. $\left(\text{Similar considerations can be used to find } M\binom{1,a,b}{f,g,h}.\right)$

Strain energy stored in stringers.- The strain energy stored in the stringers because of bending in the radial direction is

$$U_{str_r} = \sum_i (1/2)(EI)_{str_r} \int_0^L \left(\partial^2 w_r/\partial x^2\right)^2 dx \tag{8}$$

where the summation is extended over all the stringers contained in the bulge. Substitution and integration yield

$$U_{str_r} = (1/2)\left(\pi^4/L^3\right) a_o^2 \sum_i (EI)_{str_r} \left[2\Phi_{r_i}^2(1,a,b) + \left(\frac{441}{64}\right)\Phi_{r_i}^2(c,d,e) \right.$$

$$+ \left(\frac{232375}{1638\mathrm{4}}\right)\Phi_{r_i}^2(f,g,h) + \left(\frac{15}{4}\right)\Phi_{r_i}(1,a,b)\Phi_{r_i}(c,d,e)$$

$$\left. + \left(\frac{105}{32}\right)\Phi_{r_i}(1,a,b)\Phi_{r_i}(f,g,h) + \left(\frac{18315}{1024}\right)\Phi_{r_i}(c,d,e)\Phi_{r_i}(f,g,h) \right] \tag{9}$$

The strain energy stored in the stringers because of bending in the tangential direction is

$$U_{str_t} = \sum_i (1/2)(EI)_{str_t} \int_0^L \left(\partial^2 w_t/\partial x^2\right)^2 dx \tag{10}$$

Substitution and integration yield

$$U_{str_t} = (1/2)\left(\pi^4/L^3\right)\left(a_o/n\right)^2 \sum_1 (EI)_{str_t} \left[2\Phi_{t_i}^2(1,a,b) + \left(\frac{441}{64}\right)\Phi_{t_i}^2(c,d,e)\right.$$

$$+ \left(\frac{232375}{1638\mathrm{4}}\right)\Phi_{t_i}^2(f,g,h) + \left(\frac{15}{4}\right)\Phi_{t_i}(1,a,b)\,\Phi_{t_i}(c,d,e)$$

$$\left. + \left(\frac{105}{32}\right)\Phi_{t_i}(1,a,b)\,\Phi_{t_i}(f,g,h) + \left(\frac{18315}{1024}\right)\Phi_{t_i}(c,d,e)\,\Phi_{t_i}(f,g,h)\right] \qquad (11)$$

Because both the Φ functions and $(EI)_{str_r}$ and $(EI)_{str_t}$ vary from stringer to stringer, the summations appearing in equations (9) and (11) have to be evaluated numerically.

Strain energy of shear stored in sheet.- The shear strain energy per unit volume is taken as the average effective shear modulus G_{eff} multiplied by one-half the square of the average shear strain γ in the panel. The latter is calculated from the displacements of the four corners of the panel. Then the total strain energy of shear stored in the sheet is

$$U_{sh} = (1/2)\sum \gamma^2 G_{eff} L_1 td \qquad (12)$$

where L_1td is the volume of a panel.

The effective shear modulus depends upon the geometric and mechanical properties of and the average normal strain in the panel. Its value was taken from the empirical curves established earlier at PIBAL and presented in figure 24 of reference 10.

The average angle of shear γ was calculated from the equation

$$\gamma = (1/L_1)\left[\alpha_r\left(-w_{r_{i,j}} + w_{r_{i+1,j}} + w_{r_{i,j+1}} - w_{r_{i+1,j+1}}\right)\right.$$

$$+ |\alpha_t|\left(-w_{t_{i,j}} - w_{t_{i+1,j}} + w_{t_{i,j+1}} + w_{t_{i+1,j+1}}\right)$$

$$\left. + |\alpha_n| d\left(-w_{n_{i,j}} - w_{n_{i+1,j}} + w_{n_{i,j+1}} + w_{n_{i+1,j+1}}\right)\right] \qquad (13)$$

where the first subscript refers to the circumferential location and the second to the axial location of the corner of the panel, as shown in figure 3. The rotation w_n of the tangent of the ring is given by the relation

$$w_n = (1/r)\left(\partial w_r/\partial\varphi\right) \qquad (14)$$

The values of the factors α_r, α_t, and α_n were calculated from the equations

$$\left.\begin{aligned} \alpha_r &= \beta\left(0.1 + 0.000238\beta^2\right) \\ \alpha_t &= -0.5\left(1 - 0.01666\ldots\beta^2\right) \\ \alpha_n &= -(1/\beta)\left(0.5 + \alpha_t\right) \end{aligned}\right\} \qquad (15)$$

Substitutions yield

$$U_{sh} = (1/2)\, a_o^2 (td/I_1) G_0 \sum_{j=0}^{m} 2 \sum_{i=0}^{\frac{s}{2}-1} (G_{eff}/G_0) \left\{ \left[\sin^2 \frac{\pi j}{m+1} - \sin^2 \frac{\pi(j+1)}{m+1} \right] Q_i(l,a,b) \right.$$

$$\left. + \left[\sin^6 \frac{\pi j}{m+1} - \sin^6 \frac{\pi(j+1)}{m+1} \right] Q_i(c,d,e) + \left[\sin^{10} \frac{\pi j}{m+1} - \sin^{10} \frac{\pi(j+1)}{m+1} \right] Q_i(f,g,h) \right\}^2 \qquad (16)$$

where $\frac{s}{2}$ is the number of stringer fields involved in one-half of the symmetric bulge. The meaning of the symbol $Q_i(c,d,e)$ is

$$Q_i(c,d,e) = \alpha_r \left[- \Phi_{r_i}(c,d,e) + \Phi_{r_{i+1}}(c,d,e) \right] + \left(|\alpha_t| / n \right) \left[\Phi_{t_i}(c,d,e) + \Phi_{t_{i+1}}(c,d,e) \right]$$

$$+ |\alpha_n| (d/r) n \left[- (1/n)\, \Phi_{r_i}'(c,d,e) - (1/n) \Phi_{r_{i+1}}'(c,d,e) \right] \qquad (16a)$$

It is possible but cumbersome to sum up the trigonometric functions describing the deflected shape in the axial direction contained in equation (16). It was found more convenient to carry out these summations numerically. The same practice was followed as regards the Φ functions.

Work Done by External Forces

Equal and opposite forces are assumed to be acting at the x = 0 and x = L ends of each stringer. The distance between the points of application of these forces shortens at buckling. The product of this shortening and the force is the work done by the force. The total external work is the sum of the work done by the forces acting on each stringer contained in the bulge:

$$W = (1/2) \sum_i P_i \int_0^L \left[\left(\partial w_r / \partial x \right)^2 + \left(\partial w_t / \partial x \right)^2 \right] dx \qquad (17)$$

The axial strain distribution is assumed to be linear. Then P_i, the external force acting upon the ith stringer at buckling, may be expressed in terms of the buckling strain ϵ_{cr} of the most highly compressed stringer and is:

$$P_i = (EA)_i \left(\frac{\delta + \cos \varphi}{\delta + 1} \right) \epsilon_{cr} \qquad (17a)$$

where $r\delta$ is the shift of the neutral axis at buckling. Substitutions and integration yield:

$$W = (1/2)\, a_o^2 (\pi^2/L)\, \epsilon_{cr} \sum_i (EA)_i \left(\frac{\delta + \cos\Phi}{\delta + 1}\right) \left\{(1/2)\left[\Phi_{r_i}^2(1,a,b) + (1/n)^2\, \Phi_{t_i}^2(1,a,b)\right]\right.$$

$$+\left(\frac{189}{256}\right)\left[\Phi_{r_i}^2(c,d,e) + (1/n)^2\, \Phi_{t_i}^2(c,d,e)\right] + \left(\frac{60775}{65536}\right)\left[\Phi_{r_i}^2(f,g,h) + (1/n)^2\, \Phi_{t_i}^2(f,g,h)\right]$$

$$+\left(\frac{15}{16}\right)\left[\Phi_{r_i}(1,a,b)\, \Phi_{r_i}(c,d,e) + (1/n)^2 \Phi_{t_i}(1,a,b) \Phi_{t_i}(c,d,e)\right]$$

$$+\left(\frac{105}{128}\right)\left[\Phi_{r_i}(1,a,b)\Phi_{r_i}(f,g,h) + (1/n)^2 \Phi_{t_i}(1,a,b)\Phi_{t_i}(f,g,h)\right],$$

$$\left.+\left(\frac{6435}{4096}\right)\left[\Phi_{r_i}(c,d,e)\Phi_{r_i}(f,g,h) + (1/n)^2 \Phi_{t_i}(c,d,e)\Phi_{t_i}(f,g,h)\right]\right\} \qquad (18)$$

The summations encountered in equation (18) were performed numerically.

Calculation of Buckling Load

The buckling condition is

$$U_r + U_{str_r} + U_{str_t} + U_{sh} = W \qquad (19)$$

where the values of the strain energy quantities and of the work must be taken from equations (7), (9), (11), (16), and (18). Equation (19) was solved for ϵ_{cr}, which is a multiplying factor in the expression for W, and the result minimized by means of the following procedure.

Integral values of s and (m + 1) first were chosen for the number of stringer and ring fields included in the bulge. On the basis of these tentative values the Φ, M, and Q functions reduced to quadratic expressions of the eight parameters a to h. Next ϵ_{cr} was assumed; this permitted the calculation of the shift of the neutral axis, the effective widths of sheet (taken to act with the stringers), and the moments of inertia of the stringers and made it possible to read the values of (G_{eff}/G_0) from the appropriate graph. All necessary summations were then carried out. Substitution of all the results in equation (19) made it possible to obtain a solution for ϵ_{cr} in the form:

$$\epsilon_{cr} = \frac{p_1\ (1,a,b,c,d,e,f,g,h)}{p_2\ (1,a,b,c,d,e,f,g,h)} \tag{20}$$

where p_1 and p_2 are quadratic polynomials in the eight parameters a to h. Minimizing this expression for ϵ_{cr} with respect to each of these eight parameters is equivalent to setting

$$\epsilon_{cr} = \frac{p_1}{p_2} = \frac{\partial p_1/\partial a}{\partial p_2/\partial a} = \frac{\partial p_1/\partial b}{\partial p_2/\partial b} = \cdots = \frac{\partial p_1/\partial g}{\partial p_2/\partial g} = \frac{\partial p_1/\partial h}{\partial p_2/\partial h} \tag{21}$$

where the partial differential coefficients of p_1 and p_2 are linear functions of the eight parameters. Equation (21) represents nine connections between ϵ_{cr} and the eight parameters. They were solved by a trial-and-error procedure. First a value of ϵ_{cr} was assumed, and a set of values of the eight parameters was determined by solving eight linear equations. These values were substituted into the original quadratic expression to obtain a calculated value for ϵ_{cr}. This procedure was repeated with new assumptions for ϵ_{cr} until the calculated value was reasonably close to the one assumed. In order to locate the absolute minimum value of ϵ_{cr}, it is necessary to perform the calculations for a number of different choices of s and (m + 1). An example of the numerical calculations is shown in the appendix.

COMPARISON OF THEORY AND EXPERIMENT

The theory was applied to four monocoque cylinders tested earlier at GALCIT (references 4 to 8) and PIBAL (references 16 and 21). Dimensions of the cylinders showing rings and stringers are given in figure 4. Typical buckling patterns obtained in the calculations are shown in figure 2, and a tabulation of the numerical results is presented in table II. Theoretical and experimental strains rather than bending moments are compared because of the following reasoning. It was found in the calculations that the buckling strain remains practically constant if a normal strain distribution differing materially from linearity rather than a linear normal strain distribution is assumed to exist at buckling. This is so since the most highly compressed stringer ($\varphi = 0$) contributes mainly to the bending and work terms and also since the other strain energies are little affected by changes in the strain distribution. Although the critical strain is little affected by changes in strain distribution, the value of the bending moment may vary considerably. In order to calculate the latter, it is thus necessary to know the strain profile existing at buckling. Such knowledge was not available for the GALCIT cylinders. It was found convenient to assume a linear strain distribution for the PIBAL cylinders as well as for these.

The axial wave length predicted by theory for PIBAL cylinder 11 was larger than the total length of the test specimen. It was found experimentally in references 4 to 8 that if the length of a cylinder is at least twice its diameter its buckling load is independent of its length. This is not quite true for PIBAL cylinder 11 but the effect of the smaller length should be unimportant.

The four cylinders were so chosen as to cover the widest possible range in physical properties and to obtain critical stresses below or not far in excess of the proportional limit. The latter requirement was set up in order to prevent the variation in the effective modulus from attaining major importance. As may be seen from table II the theoretical buckling strains are greater than the corresponding experimental values as they should be when the strain energy method is used. The deviation is small; it amounts to 22.9 percent of the experimental value in the worst case and to 8.3 percent in the best case.

CONCLUSIONS

The strain energy theory developed for the calculation of the critical load for the inward bulge type of general instability was found to give critical stresses 8.3 to 22.9 percent higher than the experimental values obtained with four representative cylinders tested at GALCIT and PIBAL. This agreement is considered satisfactory for most practical applications

but it is likely that better agreement could be obtained by means of more comprehensive, or more suitable, assumptions for the deflected shape at buckling. The numerical calculations involved are too lengthy for use in structural design.

For this reason it is suggested that practical calculations be carried out with the aid of the procedure suggested in the paper entitled "General Instability of Monocoque Cylinders" by N. J. Hoff (Jour. Aero. Sci., vol. 10, no. 4, April 1943, pp. 105-114, 130) and in NACA TN No. 1499. The significance of the present investigation is twofold. First it permits the calculation of values of the parameter n, needed in the practical procedure suggested, in a region where experimental data are not available and too expensive to obtain. Moreover the satisfactory agreement between results of the present theory and experiments indicates that the general instability phenomenon is essentially a linear problem and can be calculated by means of a linear theory.

Polytechnic Institute of Brooklyn
Brooklyn, N. Y., March 3, 1947

APPENDIX

CALCULATIONS FOR GALCIT TEST CYLINDER 67

In this appendix details of the calculations performed in determining the critical strain for GALCIT cylinder 67 are shown. The geometric and mechanical properties for this cylinder are:

L_1, in.	4
r, in.	10
S	12
t, in.	0.012
A_{str}, $in.^2$	0.0324
I_r, $in.^4$	219.39×10^{-7}
$I_{str_{ro}}$, $in.^4$	374×10^{-6}
$I_{str_{to}}$, $in.^4$	563×10^{-6}
E_0, psi	10.5×10^6
G_0, psi	3.9×10^6

The reported experimental critical strain is 29.5×10^{-4}. At the outset of the calculations ϵ_{cr} is taken as 33×10^{-4}. The value of $r\delta$ is calculated to be 1.692 inches on the basis of a linear strain distribution. This permits the setting up of table A.

TABLE A

$[\epsilon_{cr} = 33 \times 10^{-4}; r\delta = 1.692 \text{ in.}]$

(1)	(2)	(3)	(4)	(5)	(6)	(7)	(8)	(9)	(10)	(11)	(12)
i	ϵ	2w	I_{str_r}	I_{str_t}	$\epsilon/(2.2 \times 10^{-4})$	G_{eff}/G_0	A_{eff}	$A_{eff}(\epsilon/\epsilon_{cr})$	E_{sec}	E_{tan}	E_{red}
0	33.00×10^{-4}	1.257	5.996×10^{-4}	----------	15	0.3575	0.04497	0.04497	10	6.65	8.25
1	29.22	1.342	6.082	25.32×10^{-4}	13.28	.3575	.04582	.04057	10.5	9.50	9.98
2	18.89	1.721	6.366	48.24	8.55	.385	.04961	.0284	10.5	10.5	10.5

TABLE B

$[s = 4]$

i	$\cos(2\pi i/4)$	$\cos(4\pi i/4)$	$\cos(6\pi i/4)$	$\cos(8\pi i/4)$	$\cos(10\pi i/4)$
0	1	1	1	1	1
1	0	-1	0	1	0
Multipliers for $\Phi_r(c,d,e)$	c	d	e	2.666...c -2.333...d+1.777...e	1.666...c -1.333...d+0.777...e
i	$\sin(2\pi i/4)$	$\sin(4\pi i/4)$	$\sin(6\pi i/4)$	$\sin(8\pi i/4)$	$\sin(10\pi i/4)$
0	0	0	0	0	0
1	1	0	-1	0	1
Multipliers for $\Phi_t(c,d,e)$	c	0.5d	0.333...e	0.666...c -0.5833...d+0.444...e	0.333...c -0.266...d+0.155...e
Multipliers for $-\Phi_r'(c,d,e)/n$	c	2d	3e	10.666...c -9.333...d+7.111...e	8.333...c -6.666...d+3.888...e

Column (1) refers to the stringer station. Column (2) is the strain at the locations of the stringers. Column (3) is the effective width of curved sheet calculated from the equation:

$$2w = (1/\epsilon)(d/r)\left\{0.3t + 1.535\left[(t/d)(\epsilon r - 0.3t)r^{1/2}\right]^{2/3}\right\} \qquad (A1)$$

Columns (4) and (5) give the moments of inertia of the stringers plus their effective width of curved sheet calculated from the equations:

$$I_{str_r} = I_{str_{ro}} + \frac{\left\{h + (t/2) - \left[(2w)^2/24r\right]\right\}^2}{(1/2wt) + (1/A)} + 0.8\left[(2w)^2/24r\right]^2 2wt \qquad (A2)$$

$$I_{str_t} = I_{str_{to}} + (1/12)(2w)^3 t \qquad (A3)$$

Column (6) indicates the ratio of the actual strain in a panel when the monocoque buckles to the buckling strain of a panel of sheet in compression calculated from Redshaw's formula:

$$\epsilon_{cr_{sh}} = (\epsilon_{ft}/2) + \sqrt{(\epsilon_{ft}/2)^2 + \epsilon_{cu}^2} = 2.2 \times 10^{-4} \qquad (A4)$$

The values of column (7) are read from figure 24 of reference 15. The entries in column (8) are given by $A_{str} + 2wt$. Those in column (9) can be computed from columns (2) and (8). If the strain in some members is above the proportional limit it is necessary to use reduced moduli of elasticity. In calculating the bending of the stringers the Von Kármán reduced modulus was used; in calculating the work of the external forces, the secant modulus was used. These values are based on the curves of reference 23 and given in columns (12) and (10) of table A.

For the evaluation of the Φ functions it is convenient to set up a tabular arrangement. For $s = 4$, it is given by table B. By using this table the polynominal $\Phi_r(c,d,e)$ for $i = 0$ is found by multiplying in each column the expressions in the row below the first double line by the numbers in the corresponding columns listed in the first row of

TABLE C

[s = 4]

i	$\Phi_r(c,d,e)$	$\Phi_t(c,d,e)$	$-\Phi_r'(c,d,e)/n$
0	5.333...c-2.666...d+3.555...e	0	0
1	2.666...c-3.333...d+1.777...e	1.333...c-0.2666...d-0.1777...e	9.333...c-6.666...d+0.888...e

TABLE D

[s = 4]

i	$Q_i(c,d,e)$
0	0.1454600 c -0.1248640 d -0.116546666...e
1	0.1454600 c +0.0847120 d -0.116546666...e

the table and adding the results of all the products. In a similar manner the polynomial for $\Phi_r(c,d,e)$ for $i = 1$ is obtained as well as the two expressions for each $\Phi_t(c,d,e)$ and $-\Phi_r'(c,d,e)/n$. The results are presented in table C.

The function $\left[-\Phi_{r_i}(c,d,e) + \Phi_{r_{i+1}}(c,d,e)\right]$ and the two others needed to calculate $Q_1(c,d,e)$ can be determined with the aid of table C by simply subtracting or adding the polynomials in adjacent rows for each column of that table. In doing this it must be remembered that all the Φ functions vanish when $i = 2$. The results are not shown here. When $S = 12$, $s = 4$, and $n = (12/4) = 3$ equation (15) gives:

$$\left.\begin{aligned} \alpha_r &= 0.052394 \\ |\alpha_t|/n &= 0.165905 \\ |\alpha_n|\,(d/r)n &= 0.006854 \end{aligned}\right\} \qquad (A5)$$

The value of $Q_1(c,d,e)$ determined from equation (16a) is recorded in table D. The other Φ and Q functions are derived by replacing c,d,e in tables A to D by 1,a,b, and f,g,h, respectively. In the theory the Φ and Q functions appear squared. It is thus necessary to square the polynomials of tables C and D. The results are not included here. The M functions are taken from table III; in this instance the ones corresponding to $n = 3$ are needed.

The next step in the calculations is to assume a value of $(m + 1)$, the number of ring fields involved in failure. The value of $(m + 1)$ was taken as 7 and the summations appearing in equations (6) and (16) were evaluated numerically. (Table I afforded a check for the former.) These results as well as the coefficients of the Φ functions for the stringer bending (equations (9) and (11)) and the external work (equation (18)) are tabulated in table IV. These numbers are then multiplied by the appropriate one of the M, Φ^2, and Q^2 functions to yield for each strain energy and for each value of i a quadratic form in the eight parameters consisting of 45 terms. These are to be found in table V. For the shear strain energy a constant value of G_{eff}/G_0 of 0.3575 is taken so that the quadratic expressions for $i = 0$ and $i = 1$ can be combined into one quadratic expression given in table V.

For purposes of calculation it is convenient to multiply each of equations (7), (9), (11), (16), and (18) by $\dfrac{10^4}{(1/2)a_o^2\,(\pi^2/L)E_{sec_0}}$, where E_{sec_0} is

the secant modulus of the most highly compressed stringer, and solve for $\epsilon_{cr} \times 10^4$ instead of ϵ_{cr}. In order to calculate p_1 and p_2 in equation (20), each row in table V must be multiplied by its appropriate factor. These are given as follows with numerical values calculated from data previously presented:

Strain energy	Multiplying factors
Ring	$\frac{L_1(m+1)}{\pi r^3}\left(\frac{E_r}{E_{sec_0}}\right) I_r \times 10^4 = 20.53$
Stringer, radial i = 0	$\left[\pi^2/L_1^2(m+1)^2\right]\left(\frac{E_{red_0}}{E_{sec_0}}\right) I_{str_{ro}} \times 10^4 = 0.06227$
i = 1	$2\left[\pi^2/L_1^2(m+1)^2\right]\left(\frac{E_{red_1}}{E_{sec_0}}\right) I_{str_{r1}} \times 10^4 = 0.15282$
Stringer, tangential i = 1	$2\left[\pi^2/L_1^2(m+1)^2\right]\left(\frac{E_{red_1}}{E_{sec_0}}\right) I_{str_{t1}} \times 10^4 = 0.07069$
Shear i = 0 and i = 1	$\left[4\ tr/\pi S(m+1)\right]\left(\frac{G_0}{E_{sec_0}}\right)\left(\frac{G_{eff}}{G_0}\right) \times 10^4 = 103.55$
Work i = 0	$A_0\left(\frac{\delta + \cos 0^\circ}{\delta + 1}\right)\left(\frac{E_{sec_0}}{E_{sec_0}}\right) = 0.04497$
i = 1	$2A_1\left(\frac{\delta + \cos 30^\circ}{\delta + 1}\right)\left(\frac{E_{sec_1}}{E_{sec_0}}\right) = 0.08520$

TABLE E

Matrix[1] for $\epsilon_{or} \times 10^4 = 35$

a	b	c	d	e	f	g	h	-RHS
692.2146826	-464.4565336	588.7416155	497.9358394	-332.9898263	-483.8773353	409.2661605	-273.4394178	-818.5987754
	343.7051960	385.9414027	-332.9898263	246.3400098	316.4808330	-273.4394178	202.2678766	540.9989481
		566.3080636	-475.9672414	305.0229474	491.3603230	-412.7507501	262.4374082	700.4413908
			404.3549833	-267.3909489	-412.7507501	351.6459548	-231.4902753	-588.7416157
				198.3617120	262.4374082	-231.4902753	172.0563584	385.9414027
					444.5869972	-372.6801402	235.4158705	575.5740447
						319.5626629	-209.1588705	-483.8773352
							156.1653638	316.4808330
								974.5640600
Values of the unknowns								
0.620032608	-0.899355851	-0.018836025	2.015640161	3.011252608	0.571555092	-0.457014134	-1.547918125	

[1]The lower part of the matrix has been omitted because of symmetry.

The expression $\epsilon_{cr} = (p_1/p_2)$ is obtained by multiplying the foregoing factors by the entries in table V term-by-term and adding. A first guess for $\epsilon_{cr} \times 10^4$ equal to 35 is made. The corresponding eight equations are contained in table E. They were solved by Crout's method (reference 24). The resulting values of the eight parameters were substituted into equation (20) to yield $\epsilon_{cr} = (p_1/p_2) = 36.79 \times 10^{-4}$. On using 34.5 as a second guess for $\epsilon_{cr} \times 10^4$, a value of 34.67 was obtained which was considered close enough to the new guess to terminate this procedure.

A graphic method may be used to determine accurately the critical strain after several steps in the approximate solution of the buckling equations have been undertaken. At buckling the value of the determinant formed by the coefficients of the eight equations with the right-hand-side elements transferred to the left-hand side must vanish. If a plot of the value of the determinants against the strains assumed at each stage is made, then the critical strain will correspond to the zero value of the determinant of this curve (extrapolated if necessary). Also the value of the determinant will be positive or negative, the sign depending on whether the assumed strain is below or above the critical strain. Justification for these statements may be found in reference 25. In this case such a procedure yielded $\epsilon_{cr} \times 10^4 = 34.4$ (see table II).

Instead of repeating the calculations for new values of $(m + 1)$, it was found more suitable to adopt the following scheme in minimizing the buckling strain in the axial direction. It can be shown that if $\Phi(1,a,b)/\Phi(c,d,e)$ and $\Phi(1,a,b)/\Phi(f,g,h)$ are independent of φ, then the ring, stringer, and shear energies divided by the external work become nearly proportional to $(m + 1)^2$, $1/(m + 1)^2$, and $(m + 1)^2\left(1 - \cos \frac{2\pi}{m + 1}\right)$, respectively. Since this requirement is approximately fulfilled, it is believed that the critical strain found by proportioning the three strain energies according to the foregoing factors will be close to the critical strain derived in the rigorous manner. This procedure is permissible provided that the critical value of $(m + 1)$ calculated in this manner is near the value for which the calculations were carried out rigorously, 7 in this instance. This method entails the assumption that the number of ring fields involved in failure is not an integral number. The transformation from $(m + 1) = 7$ to $(m + 1) = 7.63$, the approximate critical value obtained, is indicated as follows:

Strain Energy	$(m + 1) = 7$	$(m + 1) = 7.63$
Ring	207.754	247.020
Stringer, radial $i = 0$ $i = 1$	 216.256 67.735	 182.018 57.011
Stringer, tangential $i = 1$	 10.003	 8.419
Shear $i = 0$ and $i = 1$	216.226	218.734
$\sum = p_1$	717.974 $\epsilon_{cr} \times 10^4 = 34.67$	713.202 $\epsilon_{cr} \times 10^4 = 34.44$
p_2	20.709	20.709

Since the value $\epsilon_{cr} \times 10^4 = 34.4$ instead of 34.67 corresponds to critical strain for $(m + 1) = 7$, the correct critical strain for $(m + 1) = 7.63$ may be found by the following equation:

$$\epsilon_{cr} \times 10^4 = (34.44/34.67)(34.4) = 34.17 \qquad (A6)$$

As seen from table II, assuming $s = 2$ or $s = 6$ ($(m + 1) = 7$ in each case) gives values of the critical strain higher than the foregoing one obtained. Consequently 34.17×10^{-4} may be taken as the critical strain.

REFERENCES

1. Dschou, Dji-Djüän: Die Druckfestigkeit versteifter zylindrischer Schalen. Luftfahrtforschung, Bd. II, Nr. 8, Feb. 6, 1935, pp. 223-234.

2. Flügge, W.: Die Stabilität der Kreiszylinderschale. Ing.-Archiv., Bd. III, Heft 5, Dec. 1932, p. 463.

3. Taylor, J. L.: Stability of a Monocoque in Compression. R. & M. No. 1679, British A.R.C., 1935.

4. GALCIT: Some Investigations of the General Instability of Stiffened Metal Cylinders. I - Review of Theory and Bibliography. NACA TN No. 905, 1943.

5. GALCIT: Some Investigations of the General Instability of Stiffened Metal Cylinders. II - Preliminary Tests of Wire-Braced Specimens and Theoretical Studies. NACA TN No. 906, 1943.

6. GALCIT: Some Investigations of the General Instability of Stiffened Metal Cylinders. III - Continuation of Tests of Wire-Braced Specimens and Preliminary Tests of Sheet-Covered Specimens. NACA TN No. 907, 1943.

7. GALCIT: Some Investigations of the General Instability of Stiffened Metal Cylinders. IV - Continuation of Tests of Sheet-Covered Specimens and Studies of the Buckling Phenomena of Unstiffened Circular Cylinders. NACA TN No. 908, 1943.

8. GALCIT: Some Investigations of the General Instability of Stiffened Metal Cylinders. V - Stiffened Metal Cylinders Subjected to Pure Bending. NACA TN No. 909, 1943.

9. Heck, O. S.: The Stability of Orthotropic Elliptic Cylinders in Pure Bending. NACA TM No. 834, 1937.

10. Brazier, L. G.: The Flexure of Thin Cylindrical Shells and Other "Thin" Sections. R. & M. No. 1081, British A.R.C., 1926.

11. Hoff, N. J.: Instability of Monocoque Structures in Pure Bending. Jour. R.A.S., vol. XLII, no. 328, April 1938, pp. 291-346.

12. Von Kármán, Theodore, and Tsien, Hsue-Shen: The Buckling of Thin Cylindrical Shells under Axial Compression. Jour. Aero. Sci., vol. 8, no. 8, June 1941, pp. 303-312.

13. Hoff, N. J.: General Instability of Monocoque Cylinders. Jour. Aero. Sci., vol. 10, no. 4, April 1943, pp. 105-114, 130.

14. Hoff, N. J., and Klein, Bertram: The Inward Bulge Type Buckling of Monocoque Cylinders. III - Revised Theory Which Considers the Shear Strain Energy. NACA TN No. 968, 1945.

15. Hoff, N. J., and Boley, Bruno A.: The Shear Rigidity of Curved Panels under Compression. NACA TN No. 1090, 1946.

16. Hoff, N. J., Boley, Bruno A., and Nardo, S. V.: The Inward Bulge Type Buckling of Monocoque Cylinders. IV - Experimental Investigation of Cylinders Subjected to Pure Bending. NACA TN No. 1499, 1948.

17. Nissen, O.: Knickversuche mit versteiften Wellblechschalen bei reiner Druckbeanspruchung. Jahrb. 1937 der Deutschen Luftfahrtforschung, vol. I, pp. 452-458.

18. Ryder, E. I.: General Instability of Semimonocoque Cylinders. Air Commerce Bull., vol. 9, no. 10, April 15, 1938, pp. 241-246.

19. Wang, Tsun Kuei: Buckling of Semimonocoque Structures under Compression. Jour. App. Mech., vol. 9, no. 3, Sept. 1942, pp. A-117 - A-121.

20. Hoff, N. J., and Klein, Bertram: The Inward Bulge Type Buckling of Monocoque Cylinders. I - Calculation of the Effect upon the Buckling Stress of a Compressive Force, a Nonlinear Direct Stress Distribution, and a Shear Force. NACA TN No. 938, 1944.

21. Hoff, N. J., Fuchs, S. J., and Cirillo, Adam J.: The Inward Bulge Type Buckling of Monocoque Cylinders. II - Experimental Investigation of the Buckling in Combined Bending and Compression. NACA TN No. 939, 1944.

22. Wang, Tsun Kuei: General Instability of Semimonocoque Structures under Bending. Jour. Aero. Sci., vol. 13, no. 1, Jan. 1946, pp. 29-37.

23. Templin, R. L., Hartmann, E. C., and Paul, D. A.: Typical Tensile and Compressive Stress-Strain Curves for Aluminum Alloy 24S-T, Alclad 24S-T, 24S-RT, and Alclad 24S-RT Products. Tech. Paper No. 6, Aluminum Research Labs., Aluminum Co. of Am., 1942.

24. Crout, Prescott D.: A Short Method for Evaluating Determinants and Solving Systems of Linear Equations with Real or Complex Coefficients. Trans. A.I.E.E., vol. 60, 1941, pp. 1235-1240.

25. Boley, Bruno A.: Numerical Methods for the Calculation of Elastic Instability. Jour. Aero. Sci., vol. 14, no. 6, June 1947, pp. 337-348.

TABLE I

SUMMATION OF STRAIN ENERGY OVER ALL RINGS

$$\sum_{j=1}^{m} \sin^{2p}\left(\frac{\pi j}{m+1}\right)$$

p / (m+1)	1	2	3	4	5	6	7	8	9	10
-1	0	0	0	0	0	0	0	0	0	0
2	(1/2)(m+1)	1	1	1	1	1	1	1	1	1
3		(3/8)(m+1)	27/32	81/128	243/512	729/2048	2187/8192	6561/32768	19683/131072	59049/524288
4			(10/32)(m+1)	144/128	544/512	2112/2048	8320/8192	33024/32768	131584/131072	525312/524288
5				(35/128)(m+1)	625/512	2250/2048	8125/8192	29375/32768	106250/131072	384375/524288
6					(126/512)(m+1)	2278/2048	10380/8192	39330/32768	150756/131072	583338/524288
7						(462/2048)(m+1)	12005/8192	44933/32768	169099/131072	638666/524288
8							(1716/8192)(m+1)	51488/32768	194624/131072	740544/524288
9								(6435/32768)(m+1)	218781/131072	831222/524288
10									(24310/131072)(m+1)	923790/524288
11										(92378/524288)(m+1)

TABLE II

TABULATION OF RESULTS

Cylinder	s	(m + 1)	Strain used at outset	Strain used in solving equations	Sign of determinant	Magnitude of determinant	Strain, $\frac{p_1}{p_2}$	Value from graph, ϵ_{cr}	Critical (m + 1)	New ϵ_{cr}	Experimental (m + 1)	Experimental ϵ_{cr}	$\left(\frac{\epsilon_{cr} - \epsilon_{cr_{exp}}}{\epsilon_{cr_{exp}}}\right)(100)$
PIBAL				24×10^{-4}	+	2.309×10^{12}	36.86×10^{-4}						
cylinder	6	7	25×10^{-4}	25	+	1.024×10^{12}	30.75						
11				25.6	+	0.438×10^{10}	27.44	26.1×10^{-4}	9.55	22.59×10^{-4}	6	20.86×10^{-4}	8.3
PIBAL				19	-	4.925×10^{12}	20.98						
cylinder	6	7	17.5	18.7	-	1.543×10^{12}	18.79	18.6	7.95	18.13	7	16	13.3
54				18	+	8.812×10^{7}	22.48						
GALCIT				16.0	+	12.943×10^{12}	18.04	17.2	7.26	17.2	8	14	22.9
cylinder	4	7	15	16.4	+	8.316×10^{12}	18.32						
30				16.7	+	5.445×10^{12}	18.74						
GALCIT	2			35	+	----------	98.6						
cylinder	4	7	35	35	-	2.771×10^{12}	36.79						
67	4			34.5	-	5.749×10^{12}	34.67	34.4	7.63	34.17	-------	29.5	15.8
	6			40	-	-170.65×10^{12}	60.86						

TABLE III - $M \times 10^{-4}$

n	a^2, d^2, g^2 ad, ag, dg	ab, de, gh $1/2(ge + dh)$ $1/2(ae + bd)$ $1/2(ah + bg)$	b^2, e^2, h^2 be, bh, eh	a, cd, fg $1/2(cg + df)$ $1/2(ac + d)$ $1/2(af + g)$	b, ce, fh $1/2(ch + ef)$ $1/2(bc + e)$ $1/2(bf + h)$	l^2, c^2, f^2 c, f, cf
2	1.9629	-2.6628	0.9849	-4.6476	3.1521	2.7729
2.5	3.8714	-5.2521	1.944365	-9.16362	6.216645	5.467005
2.666...	4.7083643	-6.38755378	2.36517478	-11.14384979	7.56048132	6.6483359
3	6.7253340741	-9.123990123	3.379410699	-15.916029629	10.799091357	9.495229630
3.333...	9.24650181	-12.54446474	4.64728517	-21.88093464	14.84723739	13.05364357
4	16.02545	-21.74153333	8.05667222	-37.919000	25.73191666	22.62125
5	31.3757200	-42.56746666	15.7775644	-74.23455999	50.37909333	44.285440
6	54.28867036	-73.65386173	27.30298313	-128.44081481	87.16917901	76.62231482

TABLE IV
COEFFICIENTS OF M, Φ^2, AND Q^2 FUNCTIONS FOR
STRAIN ENERGY AND EXTERNAL WORK
$[(m + 1) = 7]$

Ring strain energy	$\sum\sum \sin^4(\pi j/7)$	2.625
	$\sum\sum \sin^{12}(\pi j/7)$	1.579101562
	$\sum\sum \sin^{20}(\pi j/7)$	1.218158722
	$2\sum\sum \sin^8(\pi j/7)$	3.8281249952
	$2\sum\sum \sin^{12}(\pi j/7)$	3.158203122
	$2\sum\sum \sin^{16}(\pi j/7)$	2.7424926744
Stringer strain energy	Coefficient of $\Phi^2(1,a,b)$	2
	Coefficient of $\Phi^2(c,d,e)$	6.890625
	Coefficient of $\Phi^2(f,g,h)$	14.18304443
	Coefficient of $\Phi(1,a,b)\,\Phi(c,d,e)$	3.75
	Coefficient of $\Phi(1,a,b)\,\Phi(f,g,h)$	3.28125
	Coefficient of $\Phi(c,d,e)\,\Phi(f,g,h)$	17.8857421S
Shear strain energy	$\sum\sum \left[\sin^2(\pi j/7) - \sin^2\pi(j + 1)/7\right]^2$	0.658892846
	$\sum\sum \left[\sin^6(\pi j/7) - \sin^6\pi(j + 1)/7\right]^2$	0.892954708
	$\sum\sum \left[\sin^{12}(\pi j/7) - \sin^{12}\pi(j + 1)/7\right]^2$	0.967843396
	$2\sum\sum \left[\sin^2(\pi j/7) - \sin^2\pi(j + 1)/7\right]\left[\sin^6(\pi j/7) - \sin^6\pi(j + 1)/7\right]$	1.235424088
	$2\sum\sum \left[\sin^2(\pi j/7) - \sin^2\pi(j + 1)/7\right]\left[\sin^{10}(\pi j/7) - \sin^{10}\pi(j + 1)/7\right]$	1.080996077
	$2\sum\sum \left[\sin^6(\pi j/7) - \sin^6\pi(j + 1)/7\right]\left[\sin^{10}(\pi j/7) - \sin^{10}\pi(j + 1)/7\right]$	1.816155626
External work	Coefficient of $\Phi_r^2(1,a,b) + (1/n)^2\Phi_t^2(1,a,b)$	0.5
	Coefficient of $\Phi_r^2(c,d,e) + (1/n)^2\Phi_t(c,d,e)$	0.73828125
	Coefficient of $\Phi_\gamma^2(f,g,h) + (1/n)^2\Phi_t(f,g,h)$	0.927352905
	Coefficient of $\Phi_\gamma(1,a,b)\,\Phi_\gamma(c,d,e) + (1/n)^2\Phi_t(1,a,b)\,\Phi_t(c,d,e)$	0.9375
	Coefficient of $\Phi_\gamma(1,a,b)\,\Phi_\gamma(f,g,h) + (1/n)^2\Phi_t(1,a,b)\,\Phi_t(f,g,h)$	0.8203125
	Coefficient of $\Phi_\gamma(c,d,e)\,\Phi_\gamma(f,g,h) + (1/n)^2\Phi_t(c,d,e)\,\Phi_t(f,g,h)$	1.571044921

TABLE V

QUADRATIC FORM IN a,b,c,d,e,f,g, AND h

$[g = 12;\ s = 4;\ (m + 1) = 7]$

Strain energy	i	Constant	a^2	b^2	c^2	d^2	e^2	f^2	
Ring		24.924977779	17.654019445	8.870953085	14.99393194	10.619996069	5.336432713	11.566696791	
Stringer, radial	0	56.888888889	14.222222222	25.2839506	196	49	87.111111111	403.4288193	
	1	14.222222222	22.222222222	6.32098766	49	76.5625	21.777777778	100.8572048	
Stringer, tangential	1	3.555555556	0.142222222	.06320988	12.25	0.49	0.217777778	25.214301212	
Shear		.0278825156	.0150011066	.01789964 84	.0377873637	.0203300261	.02425823 17	.0409564 45	
Work	0	14.222222222	3.555555556	6.320987655	21	5.25	9.333333333	26.37803818	
	1	3.65432099	5.559506175	1.582002745	5.395833337	8.208958337	2.335925928	6.777690372	
		g^2	h^2	ab	2ac	ad	2ae	2af	
Ring		8.192532482	4.116658618	-23.950474073	-60.928550848	25.745444991	-34.927774644	-50.266034467	
Stringer, radial	0	100.8572048	179.3016975	-37.925925925	-106.666666667	26.666666667	-71.111111111	-93.333333333	
	1	157.5893825	44.8254244	-23.703703703	-66.666666667	41.666666667	-44.444444444	-58.333333333	
Stringer, tangential	1	1.008572048	0.448254268	0.189629629	-2.666666667	0.266666667	0.355555556	-2.333333333	
Shear		.0220350274	.0262926766	.0061666862	-.0144310132	.02812707 49	.0115625366	-.0126271366	
Work	0	6.5945095	11.723572556	-9.481481481	-26.666666667	6.666666667	-17.777777778	-23.333333333	
	1	10.31124840	2.934196826	-5.920658435	-16.740740738	10.424074078	-11.101234566	-14.648148145	
		ag	2ah	2bc	2bd	be	2bf	2bg	hh
Ring		21.239992125	-28.815414092	41.340271559	-34.927774644	12.936806565	34.105724038	-28.815414092	10.67286542
Stringer, radial	0	23.333333333	-62.222222222	142.222222222	-71.111111111111	47.407407407	124.444444444	-62.222222222	41.481481481
	1	36.458333333	-38.888888889	35.555555556	-44.444444444	11.851851851	31.111111111	-38.888888889	10.37037037
Stringer, tangential	1	0.233333333	0.311111111111	-1.777777778	0.355555556	0.118518525	-1.555555556	0.311111111111	0.103703703
Shear		.0246111905	.0101172196	-.0837759762	.0115625366	.0335618409	-.0733039792	.0101172196	.0293666108
Work	0	5.833333333	-15.555555556	35.555555556	-17.777777778	11.851851851	31.111111111	-15.555555556	10.37037037
	1	9.121064818	-9.713580245	8.839506169	-11.101234566	2.966255147	7.734567898	-9.713580245	2.595473254

NACA

TABLE V

QUADRATIC FORM IN a,b,c,d,e,f,g, AND h - Concluded

$[s = 12;\ s = 4;\ (n + 1) = 7]$

Strain energy	i	cd	ce	cf	2cg	2ch	de	2df	
Ring		-85.13027248	17.058862030	26.040597698	-43.649594657	29.616488932	-14.407707093	-43.649594657	
Stringer, radial	0	-196.0	261.333333333	508.75	-508.75	678.333333333	-130.666666666	-508.75	
	1	-122.5	65.333333333	127.1875	-317.96875	169.583333333	-81.666666667	-317.96875	
Stringer, tangential	1	-4.9	-3.266666667	31.796875	-12.71875	-8.479166667	0.653333333	-12.71875	
Shear		-.0104306822	-.060598610	.076854663	-.021814550	-.123156260	.008357310	-.021814550	
Work	0	-21.0	28.0	44.6875	-44.6875	29.983333333	-14.0	-44.6875	
	1	-13.183333333	6.961111111	11.482204868	-28.053819423	14.189076689	-8.742222222	-28.053819423	
		dg	2dh	2df	2dg	eh	fg	fh	gh
Ring		18.444197718	-25.022476070	29.616488932	-25.022476070	9.268009084	-19.388290318	13.155007326	-11.114468148
Stringer, radial	0	127.1875	-339.166666666	678.333333333	-339.166666666	226.111111111	-403.438819279	537.9030965	-268.958246186
	1	198.730469	-211.979166	169.583333333	-211.979166	56.527777778	-252.143012	134.476273	-168.095341
Stringer, tangential	1	1.271875	1.695833333	-8.479166667	1.695833333	0.564277778	-10.085772048	-6.73981365	1.3447687
Shear		.04134872	.016997698	-.123156260	.016997698	.049338140	-.011305398	-.065630925	.009058205
Work	0	11.171875	-29.791666666	59.583333333	-29.791666666	19.861111111	-26.576045186	35.170717586	-17.587358879
	1	17.468467679	-18.603240727	14.813078689	-18.603240727	4.970794735	-16.559546192	8.743831173	-10.961079598
		a	b	c	2d	2e	f	2g	2h
Ring		-41.777277776	28.347614812	36.348988880	-60.928790844	41.340271947	29.986863862	50.866054464	34.109784098
Stringer, radial	0	-56.888888888	75.851851851	106.666666666	-106.666666666	148.222222222	93.333333333	-99.333333333	124.444444444
	1	-35.777777777	18.962962962	26.666666666	-66.666666667	39.777777778	23.333333333	-58.333333333	31.111111111
Stringer, tangential	1	-1.422222222	-0.948148148	6.666666666	-2.666666666	-1.777777778	5.833333333	-2.333333333	-1.555555555
Shear		-.007696940	-.044680321	.032279727	-.014431013	-.083775976	.049744752	.016647137	-.073309979
Work	0	-14.222222222	18.962962962	26.666666666	-26.666666666	39.777777778	29.333333333	-23.333333333	31.111111111
	1	-8.988389506	4.714403292	6.851851852	-16.740740741	8.859506189	5.995370370	-14.648148148	7.734567898

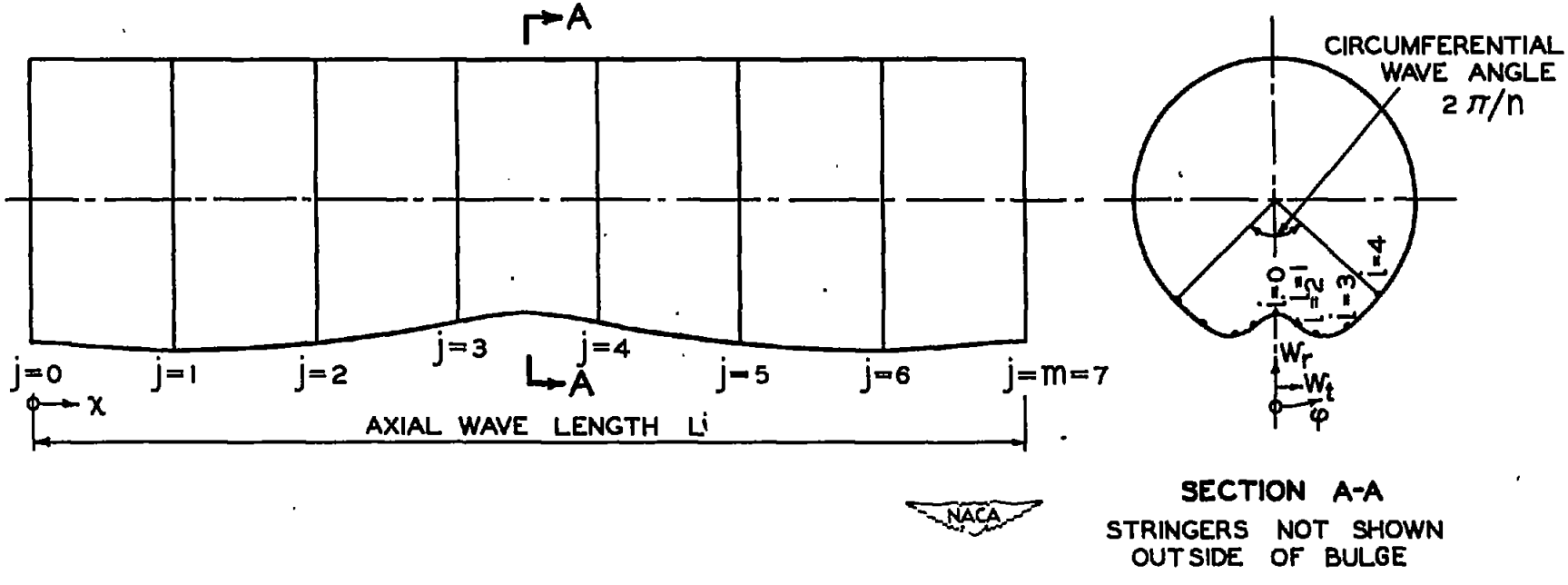

FIGURE 1.- THEORETICAL DEFLECTED SHAPE.

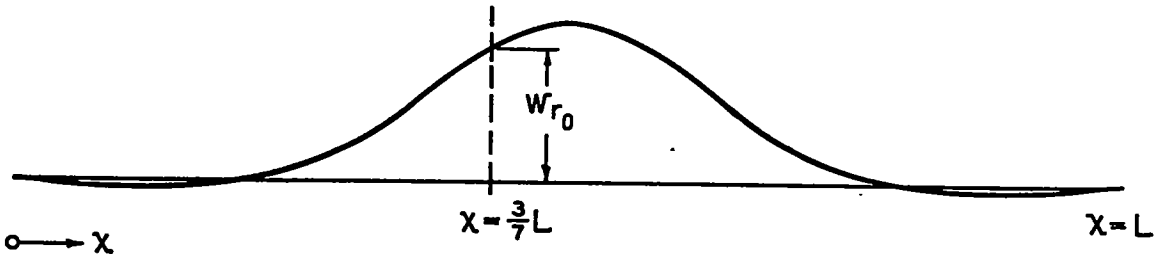

(a) BOTTOM STRINGER. $\varphi = 0$.

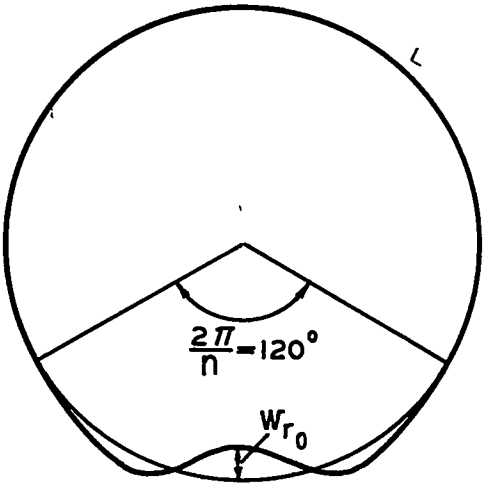

(b) RING AT $x = \frac{3}{7}L$.

FIGURE 2.- TYPICAL DEFLECTION PATTERNS. GALCIT CYLINDER 67. $S = 12$, $s = 4$, $(m + 1) = 7$.

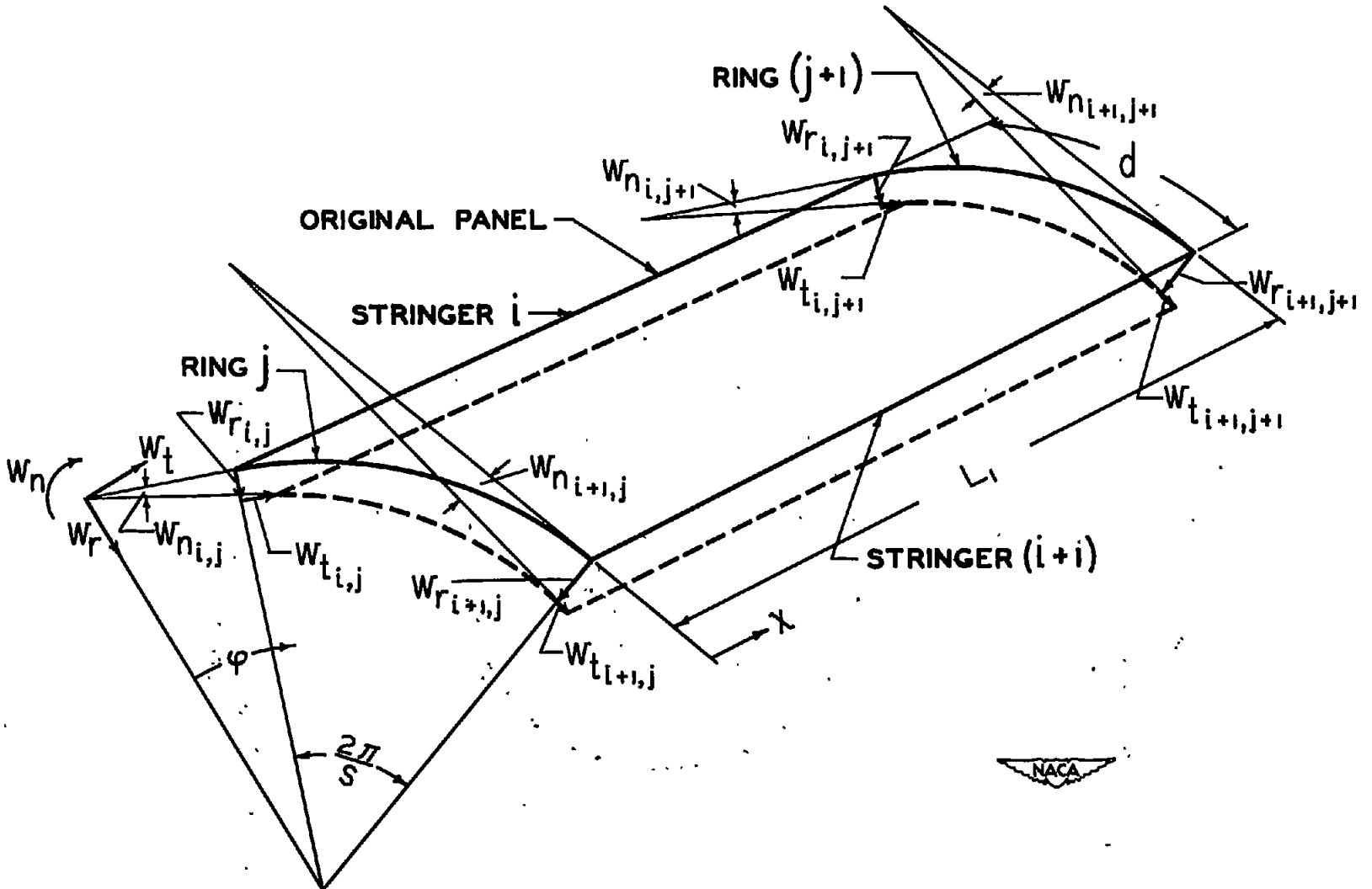

FIGURE 3.- DEFORMATION OF CORNERS OF A PANEL SHOWING NOTATION USED IN CALCULATING SHEAR STRAIN.

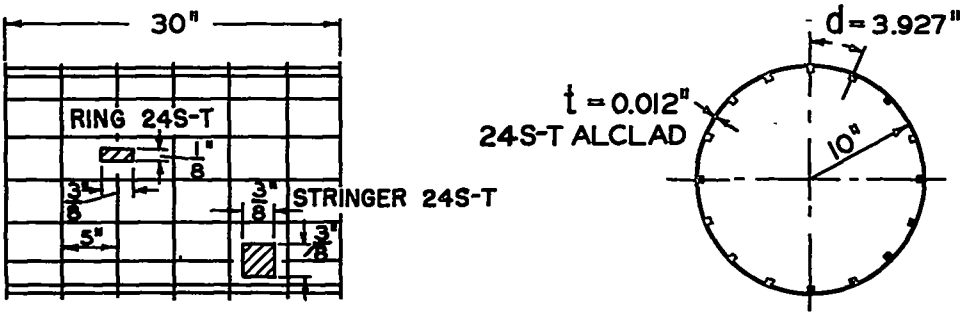

PIBAL CYLINDER 11

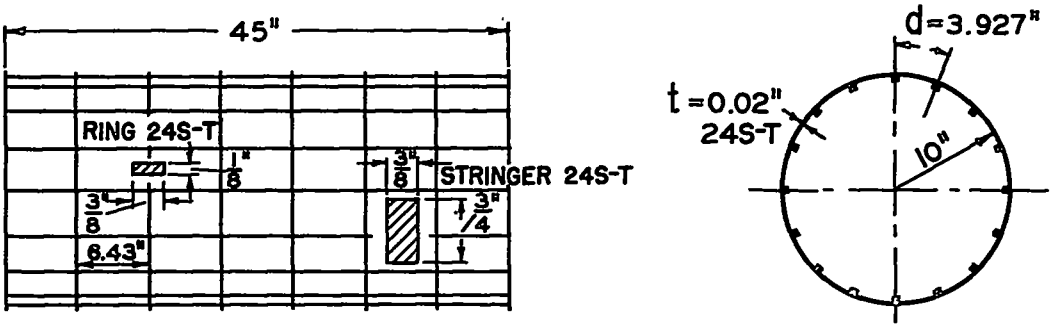

PIBAL CYLINDER 54

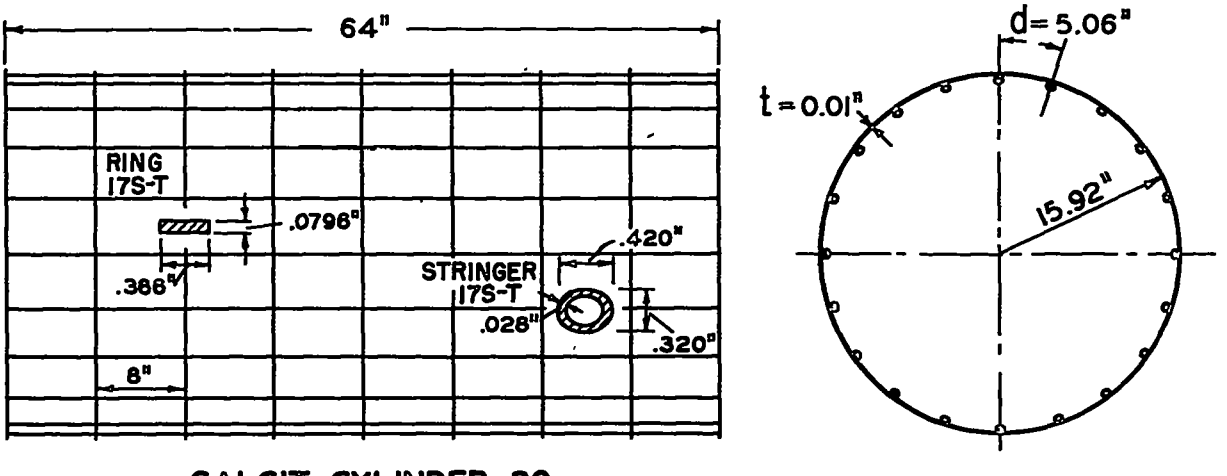

GALCIT CYLINDER 30

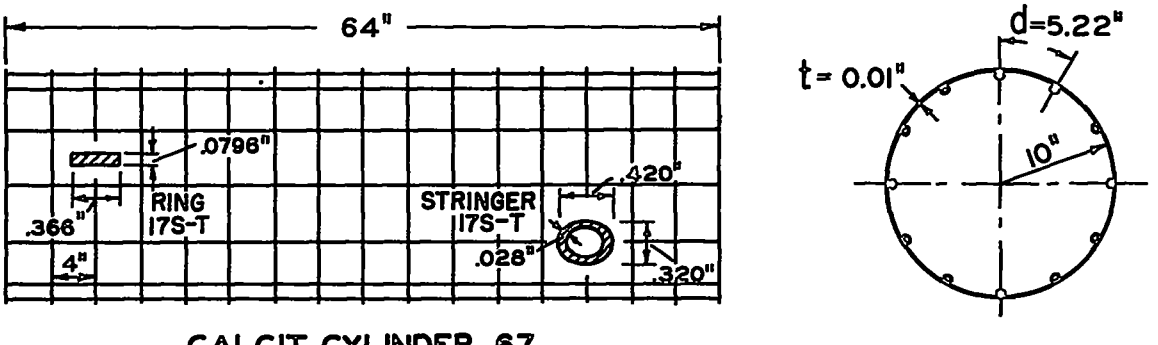

GALCIT CYLINDER 67

NACA

FIGURE 4.- MONOCOQUE CYLINDERS.